Additional insight may be gained through further Raman studies. It is interesting to note that the $\sigma^*_{Fe-N_{His}} \leftrightarrow \pi^*_{por}$ and $\pi_{His} \leftrightarrow d\pi(Fe) \leftrightarrow \pi^*_{por}$ coupling schemes are orthogonal and will be expressed through different components of the polarizability tensor: α_{xx} and α_{yy}, respectively ($N_1 - N_3$ defines the x axis, Figure 12C). Each mechanism should couple asymmetrically to the x- and y-polarized transition moments and give rise to $\rho = 0.125 - 0.33$ depending on their relative balance. More careful measurements of the polarization properties of the resonant scattering of the $Fe-N_{His}$ mode may help us to clarify this point.

Finally, it should be emphasized that our hypothesis predicts little or no Soret coupling to the $Fe-N_{His}$ mode if $\theta \rightarrow 0$. In fact, this prediction appears to be largely realized in the model compound studies of Hori and Kitagawa.[55] In this Raman investigation of $Fe^{2+}(T_{PivP}PP)$(1-MeIm) and $Fe^{2+}(T_{PivP}PP)$(2-MeIm) and their oxy complexes we see almost no scattering intensity due to the $Fe-N_{His}$ mode in the symmetric ($\theta \simeq 0$) 1-MeIm complex when compared to the asymmetric ($\theta \simeq 10°$) 2-MeIm complex.[56] (However, there is some question as to whether the iron atom in the 1-MeIm complex is actually 5-coordinate as claimed.[55]) This observation suggests that the observed Raman scattering of the 220-cm^{-1} mode in the deoxy R-state Hb and Mb results from the $\theta \neq 0$ condition. If $d\pi(Fe)$ or non-bonding repulsive interactions were responsible, we might expect them to be operative regardless of the value of θ.

It remains to be seen whether the above hypothesis will hold up to further scrutiny. One of the most interesting questions raised so far involves the observation of a strong $Fe-N_{His}$ vibration in the 10-ns photolyzed transient species of R-state Hb.[45] In order for this observation to be consistent with the arguments given above, one must assume that, after photolysis, both the iron and histidine relax rapidly (within picoseconds)[45b] to an out-of-plane configuration with $\theta \neq 0$. Model building suggests that the rapid histidine motion away from the heme plane, parallel to the z axis, may indeed be coupled to a change in polar angle (if the F helix is held fixed, rotation about the methylene carbon-α carbon bond will lead to strong coupling of the z and θ motions). The azimuthal relaxation must then proceed on a much slower time scale and presumably involves coupling to the bulk F-helix motion. In any case, we suggest that the azimuthal parameter, ϕ, must be given important consideration in any local analysis of cooperativity since the steric repulsions that play such an important role in many of the current models must also be affected by this crucial degree of freedom. In fact, it is probably a combination of steric and electron delocalization effects (as modulated by θ, ϕ, and the out-of-plane displacement) that determines the local energetics and the $Fe-N_{His}$ bond strength. Perhaps molecular dynamics simulations can ultimately help us to understand this intriguing problem in more detail.

C. Summary. We have presented the first Raman excitation profiles of the $Fe-N_{His}$ modes of deoxy Mb and deoxy Hb. We have utilized a Kramers-Kronig transform analysis to find that these modes are relatively strongly coupled $S = [0.06 - 0.16]$ to the Soret resonance. The large uncertainty in the value of S arises primarily from a lack of quantitative information about inhomogeneous conformational effects in these systems. Nevertheless, further work on this problem utilizing both the REP (1357-cm^{-1} mode) and absorption band shapes promises to help quantify the magnitude of the conformational broadening.[57] The technique of inverse transformation of REP line shapes has also been presented in order to demonstrate how careful resonance Raman measurements can resolve overlapping and congested electronic absorption spectra. In addition, we have discussed how the opposite phasing of the Condon scattering amplitude leads to discrimination against the observation of low-frequency vibrations. The observed blue shift of the REP of the 150-cm^{-1} feature remains unexplained and could conceivably be attributed to an underlying charge-transfer transition. Careful polarization studies may help to resolve this possibility. Finally, we have presented a new hypothesis that explains the coupling of the $Fe-N_{His}$ mode to the Soret resonance as well as numerous other Raman observations.

Acknowledgment. This work is supported by grants from the National Institute of Health (AM30714), the Research Corporation, and the National Science Foundation (PRM-8213711). One of us (P.M.C.) acknowledges helpful conversations with J. M. Friedman, T. G. Spiro, and K. S. Suslick.

(55) Hori, H.; Kitagawa, T. *J. Am. Chem. Soc.* **1980**, *102*, 3608-3613.
(56) Collman, J. P.; Brauman, J. I.; Rose, E.; Suslick, K. S. *J. Am. Chem. Soc.* **1978**, *100*, 6769-6770.
(57) Bangcharoenpaurpong, O.; Champion, P. M., in preparation.

Calcium-Binding Proteins: Calcium(II)-Lanthanide(III) Exchange in Carp Parvalbumin

Thomas C. Williams,* David C. Corson, and Brian D. Sykes

Contribution from the MRC Group on Protein Structure and Function and the Department of Biochemistry, University of Alberta, Edmonton, Alberta, Canada T6G 2H7.
Received December 23, 1983

Abstract: The CD and EF calcium(II)-binding sites of carp parvalbumin differ not only structurally but also functionally: one domain shows significant selectivity in lanthanide(III) exchange and the other does not. By analyzing the diamagnetically shifted His-26 and N-terminus acetyl ^1H NMR resonances of parvalbumin, we have determined that the selective site is the CD metal-ion-binding domain. The nonselective site is the EF domain. This site-dependent lanthanide selectivity of parvalbumin was further corroborated by determination of its CD- and EF-domain affinities for cerium(III), a paramagnetic lanthanide ion: $K^{CD}_{D,Ce} = 3.2 \times 10^{-11}$ M and $K^{EF}_{D,Ce} = 4.8 \times 10^{-11}$ M. By analogy to the metal-ion-binding properties of cryptands, we conclude that the EF-domain ligands are flexible, expanding or contracting relative to their calcium(II)-coordinating positions in response to lanthanide(III) exchange, whereas the ligand cage provided by the CD domain is rigid.

Parvalbumins are small ($M_r \simeq 12000$), highly acidic proteins noted primarily for their ability to tightly chelate two calcium(II) ions ($K_D \simeq 10^{-9}$ M).[1] X-ray crystallography of carp parvalbumin (isozyme pI 4.25) shows only five oxygen-containing ligands co-

0002-7863/84/1506-5698$01.50/0 © 1984 American Chemical Society

ordinating the EF-site calcium ion, compared with six similar liganding groups at the CD site.[2] However, it seems the calcium affinities at these two helix–loop–helix metal-ion-binding domains are either identical or controlled by positive cooperativity.[3-6]

Studies of solutions containing lanthanide-substituted forms of various parvalbumins corroborate this apparent functional similarity of the CD and EF domains. Thus, proton relaxation–enhancement experiments indicate that substitution at both sites by Gd(III) is characterized by only one binding constant ($K_{D,Gd} = 5.0 \times 10^{-11}$ M),[7] and the uniform increase in laser-induced luminescence of parvalbumin-bound Eu(III) or Tb(III) to a maximum near a lanthanide(III):parvalbumin ratio of 2 suggests that parvalbumin's two sites are filled at the same rate.[8-10] By contrast, other investigations of lanthanide(III) exchange in parvalbumin have revealed quite different behaviors for the CD and EF domains: Yb(III) titrations of the calcium(II)-loaded protein (monitored by the sequential appearance and disappearance of paramagnetically shifted ^{1}H NMR resonances)[11] or the cadmium(II)-loaded protein (monitored by the sequential loss of its two ^{113}Cd NMR resonances)[12] indicate that this lanthanide has strikingly different affinities for the two sites. Analyses of high-resolution, ^{1}H NMR-monitored titrations of carp parvalbumin with the diamagnetic lanthanides lanthanum(III) and lutetium(III) have shown that the site filled first by Lu(III) has the same affinity for La(III) and that the site which binds Lu(III) relatively poorly binds La(III) even tighter than the other site.[13,14]

Thus, the sequence in which parvalbumin's two high-affinity metal-binding sites are filled depends upon which Ln(III) ion is used. X-ray diffraction analyses of mono-Tb(III)-substituted parvalbumin crystals indicate that this particular lanthanide preferentially replaces calcium at the EF site.[8,15] Given this preference for EF-site substitution in the solid state, the sequential displacement of calcium by lanthanides in solution is similarly attributed to preferential exchange at the EF domain.[11,12,16-21] To corroborate this assumption, we measured the relative proton NMR-shift sensitivities of His-26 and the N-terminus acetyl residues to the two sequential phases of Lu(III) exchange. These residues, by virtue of their relative proximity to one site or the other, behave as probes of EF site-specific or CD site-specific exchange, respectively. In addition, parvalbumin's Ce(III) dissociation constants were determined, substantiating the metal-ion-binding characteristics of the larger lanthanides. Our findings indicate that smaller Ln(III) ions preferentially fill the EF site whereas the largest Ln(III) ions preferentially fill the CD site. The lanthanide(III) ion selectivities of the CD and EF sites are discussed in terms of ion:cavity size compatability, with particular reference to the metal-complexation characteristics of the macrobicyclic ligands known as cryptands.[22-25]

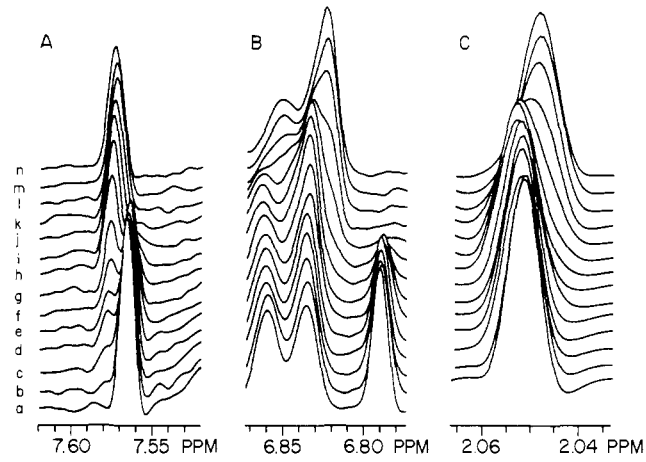

Figure 1. Lu(III)-induced shifts in the His-26 and N-terminus acetyl proton NMR resonances of carp parvalbumin (pI 4.25) at pH 6.8 and 40 °C: (A) the His-26 C_2 proton (7.565 ppm); (B) the His-26 C_4 proton (6.790 ppm; ortho protons of one Phe residue centered at 6.849 ppm); and (C) the *N*-acetyl methyl protons (2.051 ppm). The Lu(III):parvalbumin ratios are (a) 0.00, (b) 0.13, (c) 0.26, (d) 0.39, (e) 0.53, (f) 0.66, (g) 0.79, (h) 1.05, (i) 1.31, (j) 1.57, (k) 1.84, (l) 2.10, (m) 2.36, and (n) 2.62.

Experimental Section

Materials. The pI 4.25 isozyme of carp (*Cyprinus carpio*) parvalbumin was isolated by the standard method.[26] Its purity was confirmed by analysis of its characteristic phenylalanyl UV absorption maxima at λ 253, 259, 265, and 269 nm, its lack of absorbance at 280 nm, and its migration as a single band during SDS[27] gel electrophoresis and comparison of its ^{1}H NMR spectrum with standards.[28] All chemicals used were high-grade commercial products. The disodium salt of PIPES was obtained from Sigma, KCl (reagent grade) from American Scientific and Chemical, D_2O (99.75 mol %) from Bio-Rad, DSS from Merck, Sharp and Dohme, $LuCl_3 \cdot 6H_2O$ (99.9% REO purity) from Alfa Products-Ventron Division, $CeCl_3 \cdot xH_2O$ from Research Chemicals (NCA), and xylenol orange from Terochem Laboratories.

Methods. $LuCl_3$ and $CeCl_3$ solutions (50 mM) were prepared in buffered D_2O (10 mM PIPES; 100 mM KCl) and were standardized by titration against EDTA with xylenol orange as indicator.[29] Parvalbumin solutions (≃2 mM) were prepared in buffered D_2O and lyophilized twice from unbuffered D_2O, to minimize residual HDO content. Aliquots of the protein solutions were acid hydrolyzed; their amino acid content was analyzed, and parvalbumin concentrations were calculated from the alanyl and leucyl contents.

Lanthanide titrations of parvalbumin [Lu(III) at 40 °C; Ce(III) at 55 °C] were conducted with established techniques.[11,13] Proton NMR spectra were obtained with a Nicolet 300-MHz wide-bore spectrometer operating in the conventional pulsed Fourier-transform mode with qua-

(1) Goodman, M.; Pechère, J.-F.; Haiech, J.; Demaille, J. G. *J. Mol. Evol.* **1979**, *13*, 331–352.
(2) Kretsinger, R. H.; Nockolds, C. E. *J. Biol. Chem.* **1973**, *248*, 3313–3326.
(3) Potter, J. D.; Johnson, J. D.; Mandel, F. *Fed. Proc., Fed. Am. Soc. Exp. Biol.* **1978**, *37*, 1608.
(4) Benzonana, G.; Capony, J. P.; Pechère, J.-F. *Biochim. Biophys. Acta* **1972**, *278*, 110–116.
(5) Cavé, A.; Pages, M.; Morin, Ph.; Dobson, C. M. *Biochimie* **1979**, *61*, 607–613.
(6) Teleman, O.; Drakenburg, T.; Forsen, S.; Thulin, E. *Eur. J. Biochem.* **1983**, *134*, 453–457.
(7) Cavé, A.; Davres, M.-F.; Parello, J.; Saint-Yves, A.; Sempere, R. *Biochimie* **1979**, *61*, 755–765.
(8) Donato, H.; Martin, R. B. *Biochemistry* **1974**, *13*, 4575–4579.
(9) Nelson, D. J.; Miller, T. L.; Martin, R. B. *Bioinorg. Chem.* **1977**, *7*, 325–334.
(10) Rhee, M.-J.; Sudnick, D. R.; Arkle, V. K.; Horrocks, W. DeW., Jr. *Biochemistry* **1981**, *20*, 3328–3334.
(11) Lee, L.; Sykes, B. D. *Biochemistry* **1981**, *20*, 1156–1162.
(12) Corson, D. C.; Lee, L.; McQuaid, G. A.; Sykes, B. D. *Can. J. Biochem. Cell Biol.* **1983**, *61*, 860–867.
(13) Corson, D. C.; Williams, T. C.; Sykes, B. D. *Biochemistry* **1983**, *22*, 5882–5889.
(14) Williams, T. C.; Corson, D. C.; Sykes, B. D. "Calcium-binding Proteins"; de Bernard, B., et al., Eds.; Elsevier: New York, 1983; pp 57 and 58.
(15) Sowadski, J.; Cornick, G.; Kretsinger, R. H. *J. Mol. Biol.* **1978**, *124*, 123–132.
(16) Drakenburg, T.; Lindman, B.; Cave, A.; Parello, J. *FEBS Lett.* **1978**, *92*, 346–350.
(17) Horrocks, W. DeW., Jr.; Sudnick, D. R. *J. Am. Chem. Soc.* **1979**, *101*, 334–340.
(18) Lee, L.; Sykes, B. D. *Biophys. J.* **1980**, *10*, 193–210.
(19) Lee, L.; Sykes, B. D. *Biochemistry* **1980**, *19*, 3208–3214.
(20) Lee, L.; Sykes, B. D. "Biochemical Structure Determination by NMR"; Bothner-By, A. A., Glickson, J. D., Sykes, B. D., Eds.; Dekker: New York, 1982; Chapter 7, pp 169–188.
(21) Lee, L.; Sykes, B. D. *Biochemistry* **1983**, *22*, 4366–4373.
(22) Lehn, J. M.; Sauvage, J. P. *J. Am. Chem. Soc.* **1975**, *97*, 6700–6707.
(23) Gansow, O. A.; Kausar, A. R.; Triplett, K. M.; Weaver, M. J.; Yee, E. L. *J. Am. Chem. Soc.* **1977**, *99*, 7087–7089.
(24) Lehn, J. M. *Acc. Chem. Res.* **1978**, *11*, 49–57.
(25) Yee, E. L.; Gansow, O. A.; Weaver, M. J. *J. Am. Chem. Soc.* **1980**, *102*, 2278–2285.
(26) Haiech, J.; Derancourt, J.; Pechère, J.-F.; Demaille, J. G. *Biochimie* **1979**, *61*, 583–587.
(27) Abbreviations used: SDS, sodium dodecyl sulfate; PIPES, piperazine-*N*,*N*′-bis(2-ethanesulfonic acid); DSS, sodium 4,4-dimethyl-4-silapentane-1-sulfonate; FID, free-induction decay.
(28) Lee, L., Ph.D. Dissertation (Biochemistry) 1980, University of Alberta, Edmonton, Alberta, Canada T6G 2H7.
(29) Birnbaum, E. R.; Sykes, B. D. *Biochemistry* **1978**, *17*, 4965–4971.

drature detection. The spectral width was ±2000 Hz (16K points) for the Lu(III) titration series and ±3000 Hz (32K points) for the Ce(III) titration series. Each acquisition summed 2000 FIDs in double-precision format. Postacquisition processing included resolution enhancement (Lorentzian to Gaussian apodization) and zero filling. All chemical shifts were referenced to the principal resonance of DSS.

K_D Determinations. The paramagnetically shifted, minimally broadened[30] resonances generated by the Ce(III) titration of parvalbumin were used to calculate cerium's relative CD- and EF-site affinities:[11,13] resonance areas, obtained either by digital integration or curve analysis methods, were plotted as a function of the ratio of the concentration of total Ce(III) to the concentration of total parvalbumin. These curves were fitted by a least-squares routine[13] which yields, for each site, the ratio of the dissociation constant for the Ln(III) to the dissociation constant for Ca(II); to obtain comparable absolute values for the CD- and EF-site dissociation constants, the relative K_D values for Ce(III) were multiplied by the Ca(II) dissociation constant ($K_D = 4.0 \times 10^{-9}$ M).[3]

Results

Because the affinities of the CD and EF sites of parvalbumin for Ca(II) and the Ln(III) ions are very high ($\sim 10^{-9}$ M > K_D > $\sim 10^{-11}$ M) and the metal-ion-exchange rates between the metal-bound parvalbumin species are slow ($\sim 1 \times 10^{-3}$ s^{-1} < k_{off} < $\sim 1 \times 10^{-1}$ s^{-1}), the proportions of individual protein species in titration-generated mixtures of parvalbumin–metal complexes can be determined by NMR methods. For clarity, the calcium-saturated form of parvalbumin will be referred to as the Ca_2 form (or the Ca:Ca form), the two singly lanthanide-substituted forms as the Ca_1Ln_1 forms (or the Ln:Ca form if the CD site is exchanged and Ca:Ln if the EF site is exchanged), and the doubly lanthanide-substituted form as the Ln_2 form (or the Ln:Ln form).

Lutetium(III) Exchange. The relatively minor shifts in parvalbumin's diamagnetic ^{1}H NMR resonances induced by Lu(III) exchange arise from slight adjustments in the protein's tertiary conformation in response to this lanthanide's high charge density.[13,31] Each series of titration spectra (Figure 1) showed the two sequential metal-ion exchanges undergone by the Ca_2 form of parvalbumin: the first conversion yielded predominantly one of two Ca_1Lu_1 forms and the second conversion produced the final Lu_2 form. The His-26 C_2–H singlet resonance of the Ca_2 form (7.565 ppm) clearly diminished throughout the initial phase of the titration, being replaced by the resonance (7.575 ppm) of the predominant Ca_1Lu_1 form (Figure 1A). During the second phase of the titration, the conversion of parvalbumin to the Lu_2 form was manifested by a slight upfield shift in the C_2–H resonance position (7.573 ppm). Similarly, the His-26 C_4–H singlet resonance of the Ca_2 form (6.790 ppm) was replaced, during the initial phase, by a singlet resonance at 6.834 ppm. As indicated in Figure 1B, this resonance overlaps the upfield transition of a doublet resonance from the ortho protons of one of Ca_2-parvalbumin's 10 phenylalanine residues. The C_4–H singlet at 6.834 ppm was replaced, during conversion of the Ca_1Lu_1 form to the Lu_2 form, by a singlet rising at 6.823 ppm. Conversely, the singlet resonance of the *N*-acetyl group (Ca_2 form) shifted only slightly downfield, from 2.051 to 2.052 ppm, during the initial phase (Figure 1C). Conversion of Ca_1Lu_1-parvalbumin to the Lu_2 form was evidenced by the comparatively greater upfield shift of this resonance to 2.048 ppm. Comparison of the His-26 C_2–H (or C_4–H) resonance positions showed that this residue was 4–5 times more sensitive to the initial phase of Lu(III) titration, whereas comparison of the *N*-acetyl resonance showed this group to be 4 times more sensitive to the later phase of titration (Table I).

Cerium(III) Exchange. Several resonances in the ^{1}H NMR spectrum of Ca_2-parvalbumin proved particularly informative monitors of Ca(II)–Ce(III) exchange. In the *N*-acetyl region alone (Figure 2B; Table I), all four metal-bound parvalbumin species were monitored simultaneously as a function of added Ce(III). Three of the four resonances were clearly resolved as singlets of comparable line width (2.5 Hz < $\Delta\nu_{1/2}$ < 2.9 Hz): the Ca_2 form's

Table I. His-26 and *N*-Acetyl ^{1}H NMR Chemical Shifts of Selected Metal-Bound Forms of Carp Parvalbumin (pI 4.25)[a]

metal occupancy[b]	His-26,C_2	His-26,C_4	*N*-acetyl
Ca:Ca[c]	7.565	6.790	2.051
Lu:Ca			
Ca:Lu	7.575	6.834	2.052
Lu:Lu	7.573	6.823	2.048
Ca:Ca[d]	7.581		2.045
Ce:Ca	7.548		2.054
Ca:Ce			2.032
Ce:Ce			2.069

[a] In units of ppm from DSS; [parvalbumin] ~ 2 mM in 100 mM KCl, 10 mM PIPES. [b] This notation is adopted from the following convention: (CD-site occupancy):(EF-site occupancy). [c] At 40 °C; pH 6.8. [d] At 55 °C; pH 5.9.

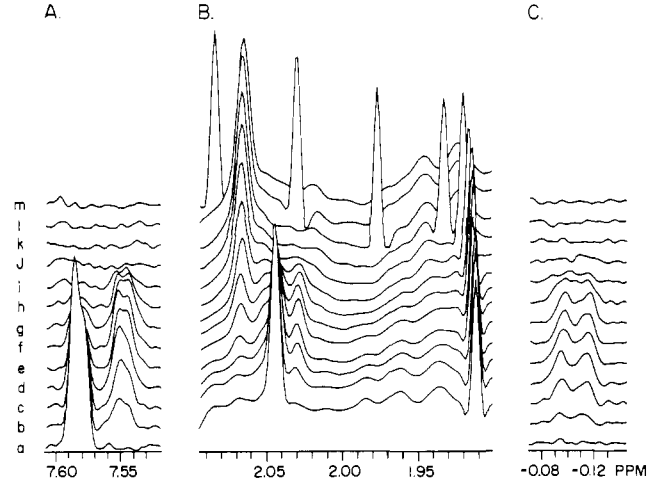

Figure 2. Selected Ce(III)-induced shifts in the ^{1}H NMR spectrum of carp parvalbumin (pI 4.25) at pH 5.9 and 55 °C: (A) the His-26 C_2 proton in the Ca:Ca form, 7.581 ppm, and in the Ce:Ca form, 7.548 ppm; (B) the *N*-acetyl methyl protons in the Ca:Ca form, 2.045 ppm, in the Ce:Ca form, 2.054 ppm, in the Ca:Ce form, 2.032 ppm, and in the Ce:Ce form, 2.069 ppm; (C) unassigned methyl protons in the Ca:Ce form, −0.105 ppm. (Free acetate is at 1.913 ppm in spectrum a.) The Ce(III):parvalbumin ratios are (a) 0.00, (b) 0.204, (c) 0.408, (d) 0.612, (e) 0.816, (f) 1.020, (g) 1.225, (h) 1.429, (i) 1.633, (j) 1.837, (k) 2.041, (l) 2.245, and (m) 2.449.

N-acetyl resonance (at 2.045 ppm) decreased in intensity throughout the titration, falling to near zero by the titration's midpoint; one intermediate Ca_1Ce_1 form was evidenced by the initial rise and subsequent fall of the less-intense singlet resonance at 2.032 ppm; and conversion to the Ce_2 form was indicated by the progressive increase in intensity of the singlet resonance at 2.069 ppm. The fourth resonance was attributed to the other intermediate Ca_1Ce_1 form and appeared as a significantly broader singlet ($\Delta\nu_{1/2}$ = 4.2 Hz) at 2.054 ppm obscured by overlap with the *N*-acetyl resonance of the Ca_2 form. Curve analyses of each set of four adjacent *N*-acetyl resonances yielded the proportions (relative integrated areas) of the individual metal-bound parvalbumin species at the given [Ce(III)] total:[parvalbumin] total ratios (Figure 3; see ref 32).

To supplement these values, the relative integrated intensities of the His-26 C_2–H resonances (at 7.581 ppm in the Ca_2 form and at 7.548 ppm in one of the intermediate Ca_1Ce_1 forms; see

(30) Lee, L.; Sykes, B. D. In "Advances in Inorganic Biochemistry"; Darnall, D. W., Wilkins, R. G., Eds.; Elsevier/North-Holland: New York, 1980, Vol. 2, pp 183–210.

(31) Matthews, B. W.; Weaver, L. H. *Biochemistry* **1974**, *13*, 1719–1725.

(32) Note: The disparity in the *N*-acetyl resonance line widths of the three different Ce(III)-bound parvalbumins (i.e., the Ca:Ce, Ce:Ca, and Ce:Ce forms) and the apparent nonadditivity of their induced paramagnetic shifts may reflect the subtle differences in protein conformation known to be generated by lanthanide exchange.[13] Since the resonance line broadening of lanthanide(III)-bound parvalbumins stems mainly from proton dipole–dipole and magnetic susceptibility contributions (i.e., the dipolar interaction of the non-zero electronic spin moment of the metal ion with the proton spin),[19] the observed differences in *N*-acetyl line widths imply that the species with the broadest resonance is either less mobile and/or closer to the metal.

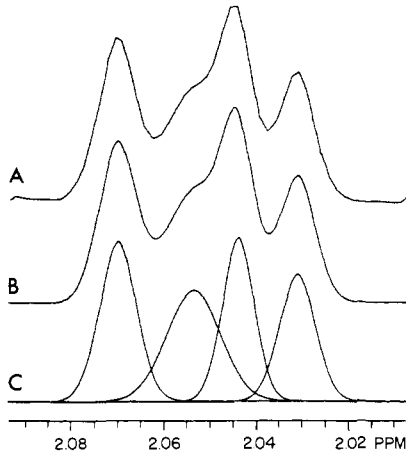

Figure 3. Curve analysis of the *N*-acetyl region of the ^{1}H NMR spectrum of carp parvalbumin. The line shape was treated as 100% Gaussian (due to the Lorentzian-to-Gaussian postacquisition apodization of the FID), and the region was base-line corrected with a linear tilt routine. The Ce(III):parvalbumin ratio is 1.020: (A) experimental spectrum (an expansion of spectrum f, Figure 2B); (B) calculated composite spectrum; (C) calculated constituent *N*-acetyl resonances. Ce:Ce form, 2.069 ppm, $\Delta\nu_{1/2}$ = 2.9 Hz; Ce:Ca form, 2.054 pm, $\Delta\nu_{1/2}$ = 4.2 Hz; Ca:Ca form, 2.045 ppm, $\Delta\nu_{1/2}$ = 2.5 Hz; Ca:Ce form, 2.032 ppm, $\Delta\nu_{1/2}$ = 2.8 Hz.

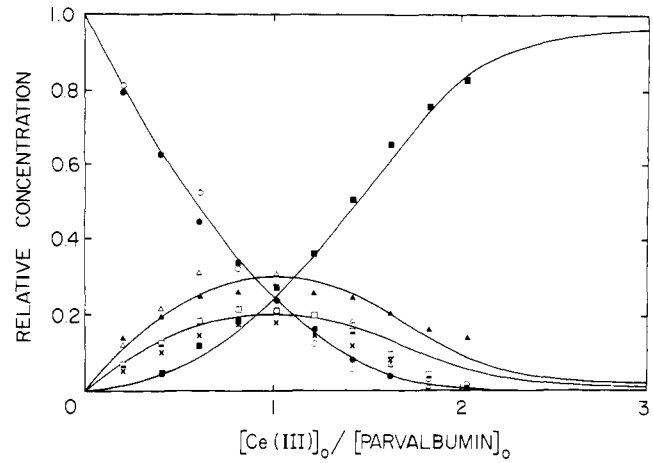

Figure 4. Ce(III) titration data of carp parvalbumin. Relative peak areas of the four *N*-acetyl resonances, two His-26 C_2–H resonances, and one unassigned methyl resonance illustrated in Figure 2 are plotted vs. the Ce(III):parvalbumin ratios listed there. Overlying the data points are the theoretical distribution curves calculated from the dissociation constants obtained by a least-squares fit of the data: (●) *N*-acetyl, Ca:Ca form; (○) His-26 C_2–H, Ca:Ca form; (▲) *N*-acetyl, Ce:Ca form; (△) His-26 C_2–H, Ce:Ca form; (□) *N*-acetyl, Ca:Ce form; (×) unassigned upfield methyl, Ca:Ce form; (■) *N*-acetyl, Ce:Ce form.

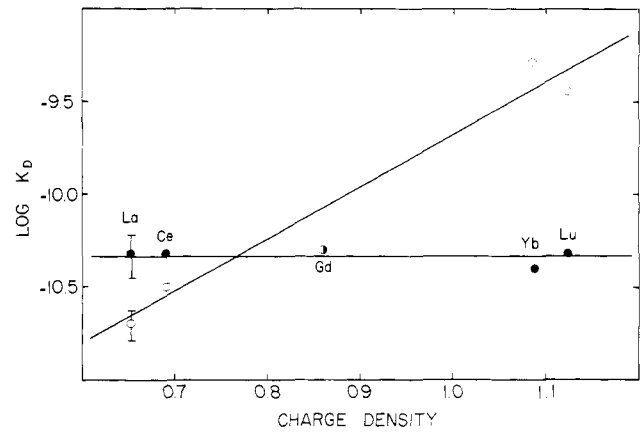

Figure 5. Logarithm K_D vs. charge density for dissociation of several Ln(III)s from carp parvalbumin. $K^{CD}_{D,Yb}$ = 5.2 × 10^{-10} M and $K^{EF}_{D,Yb}$ = 4.0 × 10^{-11} M (ref 11); $K^{CD}_{D,La}$ = 2.0 × 10^{-11} M, $K^{EF}_{D,La}$ = 4.8 × 10^{-11} M, $K^{CD}_{D,Lu}$ = 3.6 × 10^{-10} M, and $K^{EF}_{D,Lu}$ = 4.8 × 10^{-11} M (ref 13); $K^{CD}_{D,Gd}$ = $K^{EF}_{D,Gd}$ = 5.0 × 10^{-11} M (ref 7); $K^{CD}_{D,Ce}$ = 3.2 × 10^{-11} M and $K^{EF}_{D,Ce}$ = 4.8 × 10^{-11} M (this work). The charge density was taken as $\delta/[(4/3)\pi r^3]$. Radii were taken as the 6-coordinate values listed in ref 36. See ref 37.

Figure 2A and ref 33) and a particularly well-resolved, though unassigned, methyl doublet resonance at −0.105 ppm (attributed to one of the intermediate Ca_1Ce_1 species; see Figure 2C) were also determined as a function of added Ce(III). For the C_2–H resonances, integrations were made relative to the area of the C_2–H resonance of the Ca_2 form; for the unassigned methyl resonance, integrations were made relative to the area of the well-resolved methyl doublet resonance at −0.362 ppm in the spectrum of the Ca_2 form. As did the *N*-acetyl resonance of the Ca_2 form, the His-26 C_2–H resonance progressively diminished from the first addition of Ce(III). On the other hand, the resonances at 7.548 and −0.105 ppm followed the intensity trends exhibited by the Ca_1Ce_1 intermediate species, each rising to its maximum intensity at a Ce(III):parvalbumin ratio of 1 before gradually decreasing to undetectable levels.

Contaminating acetate ions gave rise to a sharp singlet resonance at 1.913 ppm. As shown in Figure 2B, this resonance, unaffected throughout most of the titration, suddenly shifted progressively downfield after near-complete conversion of parvalbumin to the Ce_2 form. This observed behavior of the free acetate resonance is characteristic of and attributed to fast exchange with Ce(III) ions.

Figure 4 illustrates the relative proportions of these resonances plotted as a function of the ratio $[Ce(III)]_{total}/[parvalbumin]_{total}$. The calculated relative dissociation constants (i.e., the $K_{D,Ce}/K_{D,Ca}$ ratios; see Experimental Section) were $K^1_{D,Ce}$ = 0.008 and $K^2_{D,Ce}$ = 0.012, the superscripts 1 and 2 indicating the two distinct dissociation constants extracted from the least-squares analysis. These K_D values were later assigned specifically to the CD and EF sites of parvalbumin. Preliminary assignments to the lanthanide selective or nonselective site were made by comparison of the Ce(III) K_D values with known carp parvalbumin Ln(III) dissociation constants. Converted to absolute values, the cerium(III) dissociation constants were $K^1_{D,Ce}$ = 3.2 × 10^{-11} M and $K^2_{D,Ce}$ = 4.8 × 10^{-11} M. Compared with the K_D values for La(III) [K^1_D = 2.0 × 10^{-11} M; K^2_D = 4.8 × 10^{-11} M],[13] Gd(III) [K^1_D = K^2_D = 5.0 × 10^{-11} M],[7] Yb(III) [K^1_D = 5.2 × 10^{-10} M; K^2_D = 4.0 × 10^{-11}],[11] and Lu(III) [K^1_D = 3.6 × 10^{-10} M; K^2_D = 4.8 × 10^{-11} M],[13] these $K_{D,Ce}$ values follow an established trend: the affinities for site 1 varied markedly over the series, whereas those for site 2 did not (Figure 5). Just as the higher affinity Yb(III) K_D was assigned[13] to the nonselective site by comparison with the La(III) and Lu(III) K_Ds, the higher affinity Ce(III) K_D was assigned to the lanthanide-selective site.

Discussion

Variations in the structure of homologous regions of a protein are commonly expressed as differences in function. For example, the two structurally distinguishable calcium(II)-binding sites of both hake (isozyme pI 4.36) and whiting parvalbumin have different affinities for this metal.[34,35] However, the carp isozyme (pI 4.25), whose CD- and EF-site amino acid sequences are nearly

(33) Note: The C_2–H and C_4–H ^{1}H NMR resonances of His-26 frequently appear as doublets, the separation of peaks within each doublet being different and dependent on pH, temperature, and magnetic field strength; homonuclear spin–spin couplings are, therefore, not the source of their doublet appearance. Similar observations have been made of the ^{1}H NMR resonances of the histidine residues (Gronenborn, A.; Birdsall, B.; Hyde, E. I.; Roberts, G. C. K.; Feeney, J.; Burgen, A. *Mol. Pharmacol.* **1981**, *20*, 145–153) and the ^{13}C NMR resonances of the γ carbons of two of the four tryptophan residues (London, R. E.; Groff, J. P.; Blakely, R. L. *Biochem. Biophys. Res. Commun.* **1979**, *86*, 779–786) in dihydrofolate reductase. As was proposed for these residues of dihydrofolate reductase, we attribute the doublet character of the histidine residue of carp parvalbumin to a slow exchange phenomenon between two conformationally nonequivalent microenvironments.

(34) Haiech, J.; Derancourt, J.; Pechere, J.-F.; Demaille, J. G. *Biochemistry* **1979**, *18*, 2752–2758.

(35) White, H.; Closset, J. *Biophys. J.* **1979**, *25*, 247a.

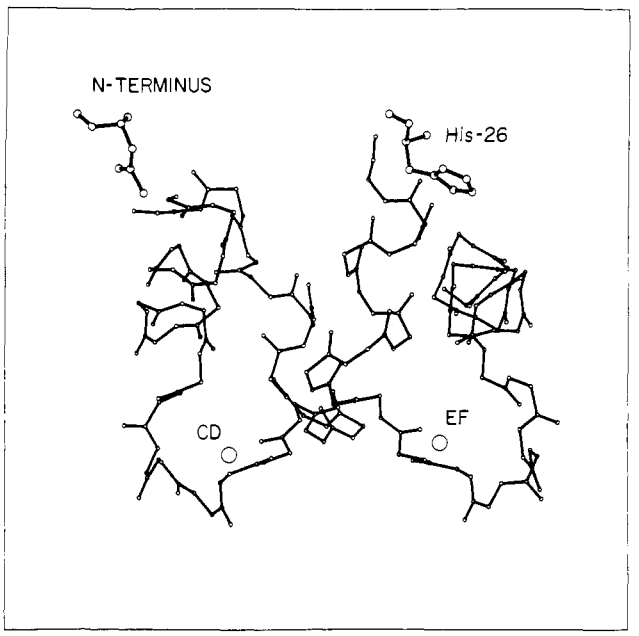

Figure 6. Ball-and-stick representation of the *N*-acetyl group and the His-26 residue, showing their relative proximities to the CD and EF metal-binding sites of carp parvalbumin. Only the main-chain atoms (C, C_α, O, N) have been used to illustrate the positions of the CD domain (residues 42–68) and the EF domain (residues 79–106). [Derived from the X-ray crystallographic coordinate set, ref 2.]

identical with those of the hake and whiting isozymes,[1] binds two Ca(II) ions with apparently equal affinities. Although the CD and EF domains of the carp isozyme appear to be functionally identical when probed by Ca(II) binding, their lanthanide(III) exchange behaviors are markedly dissimilar. Exchange of certain Ln(III) ions for the bound Ca(II) ions of the calcium-saturated form of carp parvalbumin follows a well-documented sequential mechanism:[11,14] Yb(III) and Lu(III) share a strong preference for one of the metal-binding sites (site 2), whereas La(III) and Ce(III) show slight preferences for the other (site 1). Furthermore, site 2 has essentially equal affinities for all Ln(III) ions. Conversely, site 1 is selective—i.e., it binds the smaller Ln(III) ions relatively poorly.

Assignment of the lanthanide-selective exchange behavior to either the CD or EF site required some means of monitoring the substitution at one or both domains. Because the singlet NMR resonances of the C_2 and C_4 protons of His-26 and the methyl protons of the acetylated N-terminus are assigned and well-resolved, we chose to monitor their Lu(III)-induced resonance shifts during titration of the carp isozyme (pI 4.25) to assign the selective and nonselective sites. The crystal structure of parvalbumin[2] shows the ring protons of His-26 nearer the EF than the CD site, thus serving as monitors of Lu(III) exchange at the EF domain (Figure 6): r_{EF} = 13.6 Å vs. r_{CD} = 18.8 Å for C_2–H and r_{EF} = 15.1 Å vs. r_{CD} = 18.8 Å for C_4–H. Conversely, the N-terminus is nearer the CD site, providing a probe of the exchange in this domain: r_{CD} = 14.1 Å vs. r_{EF} = 20.1 Å for the methyl protons of the *N*-acetyl function. The greater sensitivity of the His-26 resonances during the initial phase of the Lu(III) titration (Figure 1, Table I) reveals that the EF-site Ca(II) ion is exchanged first. The later filling of the CD site is evidenced by the greater sensitivity of the *N*-acetyl resonance to the second phase of the Lu(III) titration. Thus, the lanthanide-selective metal-binding domain of carp parvalbumin is the CD site and the lanthanide-nonselective metal-binding domain is the EF site.

The selectivity of cryptands (polyoxadiazamacrobicyclic ligands) for various alkaline earths, lanthanide(II), and lanthanide(III) ions (including La, Pr, Eu, Gd, and Yb) is well-documented[22-25] and serves as a useful model for the observed selectivity of the CD site of parvalbumin. These rigid macrobicyclic ligands encapsulate a metal ion in a cavity of essentially fixed radius (from about 1.1 to 1.4 Å, depending on the particular cryptand). The complexation thermodynamics of cryptates indicate that the closer the match between the size of the encapsulated ion and the cryptand's cavity, the more stable is the cryptate complex. If one assumes that the cavity of the CD metal-binding site of parvalbumin is optimally fitted to the ionic radius of Ca(II) (i.e., a cavity size of about 1.0 Å) and that its ligands are relatively inflexible (due to the complete octahedral-like coordination of the metal by protein ligands), then, by analogy to the cryptates, one would predict that the larger lanthanide(III) ions (e.g., Ce(III) whose ionic radius is 1.01 Å) would form more stable complexes than would the smaller lanthanide(III) ions (e.g., Lu(III) whose ionic radius is 0.86 Å). Designation of the CD domain as a rigid metal-binding site agrees well with our results. Conversely, the apparent lanthanide(III) nonselectivity of the EF site suggests that it is not rigid.

Conclusion

Optical stopped-flow studies[12] of the Ln(III) exchange kinetics of carp parvalbumin indicated that the metal-binding site characterized by the slower of two Yb(III) off-rate constants (k_{off}) is also that site which binds Yb(III) more tightly. Subsequent investigations[13] revealed not only that the k_{off} for this particular site increases significantly when the Ln(III) series is crossed from Lu(III) to La(III) but also that the k_{off} for the other site changes very little, decreasing slightly from Lu(III) to La(III). Because rates of lanthanide(III) complex formation (k_{on}) are primarily determined by the dehydration rate of the aquo cation, and the cross-series trend in dehydration rates parallels the increase in the k_{off} for the slow site, the dissociation constant for this site remains essentially constant across the lanthanide(III) series.[7,11,13] Conversely, the minor changes in k_{off} behavior of the other site, coupled with the indicated trend in Ln(III) dehydration rates, give that site a higher affinity for La(III) than for Lu(III).[13] We have now shown that the metal-binding site of carp parvalbumin which binds Ln(III) ions indiscriminately is the EF domain, and we suggest that its ligands are sufficiently flexible to compensate for variations in the ionic size of chelated metals. On the other hand, the CD site's strong preference for larger Ln(III) ions indicates that its chelating side chains are fixed and unable to accommodate the smaller Ln(III) ions optimally.

Acknowledgment. The authors thank M. Nattriss for the amino acid analyses of the protein samples, M. Fujinaga for constructing Figure 5, and P. McDonald and U. Matthews for preparing and critically reading this manuscript. This work was supported by the Medical Research Council Group on Protein Structure and Function and the Alberta Heritage Fund for Medical Research (Fellowship and research allowance to T.C.W.).

Registry No. Lu, 7439-94-3; Ce, 7440-45-1; Ca, 7440-70-2.

(36) Kretsinger, R. H. *Coord. Chem. Rev.* **1976**, *18*, 29–124.

(37) Note: In Figure 1 of both ref 13 and ref 14, the abscissa was incorrectly referred to as either δ/r^3 or charge density; it was, in fact, $\delta/3r^3$ where δ is the formal charge on the metal ion. These corrections, however, in no way change the apparent linearity of the observed results or the validity of the conclusions therefrom.